Pedosphere **21**(6): 719–729, 2011
ISSN 1002-0160/CN 32-1315/P

Published by Elsevier B.V. and Science Press

PEDOSPHERE

www.elsevier.com/locate/pedosphere

Grass Cover Influences Hydrophysical Parameters and Heterogeneity of Water Flow in a Sandy Soil*1

L. LICHNER[1,*2], D. J. ELDRIDGE[2], K. SCHACHT[3], N. ZHUKOVA[4], L. HOLKO[1], M. ŠÍR[5] and J. PECHO[6]

[1]*Institute of Hydrology, Slovak Academy of Sciences, Racianska 75, 83102 Bratislava (Slovakia)*
[2]*Department of Environment Climate Change and Water, School of Biological, Earth and Environmental Sciences, University of New South Wales, Sydney, NSW 2052 (Australia)*
[3]*Geography Department, Ruhr-University Bochum, Universitaetsstrasse 150, 44801 Bochum (Germany)*
[4]*M. Nodia Institute of Geophysics, 1 Alexidze str., 0193 Tbilisi (Georgia)*
[5]*Institute of Hydrodynamics, Academy of Sciences of the Czech Republic, Pod Patankou 30/5, 16612 Prague (Czech Republic)*
[6]*Institute of Atmospheric Physics, Academy of Sciences of the Czech Republic, 1401 Bocni II, 14131 Prague (Czech Republic)*

(Received April 26, 2011; revised September 23, 2011)

ABSTRACT

Vegetation cover has a major effect on water flow in soils. Two sites, separated by distance of about 50 m, were selected to quantify the influence of grass cover on hydrophysical parameters and heterogeneity of water flow in a sandy soil emerging during a heavy rain following a long hot, dry period. A control soil (pure sand) with limited impact of vegetation or organic matter was obtained by sampling at 50 cm depth beneath a glade area, and a grassland soil was covered in a 10 cm thick humic layer and colonised by grasses. The persistence of water repellency was measured using the water drop penetration time test, sorptivity and unsaturated hydraulic conductivity using a mini disk infiltrometer, and saturated hydraulic conductivity using a double-ring infiltrometer. Dye tracer experiments were used to assess the heterogeneity of water flow, and both the modified method for estimating effective cross section and an original method for assessing the degree of preferential flow were used to quantify this heterogeneity from the images of dyed soil profiles. Most hydrophysical parameters were substantially different between the two surfaces. The grassland soil had an index of water repellency about 10 times that of pure sand and the persistence of water repellency almost 350 times that of pure sand. Water and ethanol sorptivities in the grassland soil were 7% and 43%, respectively, of those of the pure sand. Hydraulic conductivity and saturated hydraulic conductivities in the grassland soil were 5% and 16% of those of the pure sand, respectively. Dye tracer experiments revealed a stable flow with "air-draining" condition in pure sand and well-developed preferential flow in grassland soil, corresponding to individual grass tussocks and small micro-depressions. The grassland soil was substantially more water repellent and had 3 times the degree of preferential flow compared to pure sand. The results of this study reinforce our view that the consequences of any change in climate, which will ultimately influence hydrology, will be markedly different between grasslands and bare soils.

Key Words: dye tracing, grassland soil, hydrophobicity, infiltration, preferential flow

Citation: Lichner, L., Eldridge, D. J., Schacht, K., Zhukova, N., Holko. L., Šír, M. and Pecho, J. 2011. Grass cover influences hydrophysical parameters and heterogeneity of water flow in a sandy soil. *Pedosphere*. **21**(6): 719–729.

INTRODUCTION

Global changes in the Earth's climate are known to have substantial and irreversible effects on soil and ecological processes (Solomon *et al.*, 2007). Climate change projections for continental Europe, for example, suggest a general increase in air temperatures and large changes in rainfall patterns (Hardy, 2003). Lenderink and van Meijgaard (2010) predicted that the hourly precipitation extremes could increase

*1Supported by the Slovak Scientific Grant Agency VEGA (Nos. 2/0042/11 and 2/0073/11) and by the Ministry of the Environment of the Czech Republic (No. VaV SP/lab/151/07).
*2Corresponding author. E-mail: lichner@uh.savba.sk.

by 70% or even more by the end of this century.

Changes to the summer precipitation regime have important implications for hydrology. Many areas of southern Slovakia are experiencing increases in the frequency and intensity of heavy rains following long hot, dry periods (Faško *et al.*, 2008), leading to increased surface runoff, soil erosion and deposition of sediment within rivers and streams, as well as a nutrient washout (Pekarova *et al.*, 1999). The relationship between rainfall intensity, runoff and infiltration capacity of the soil is clearly an important consideration for determining the amount of total catchment runoff and its components (overland flow *versus* subsurface flow) following high-intensity storms (*e.g.*, Šanda and Císlerová, 2009; Holko *et al.*, 2011).

Runoff is likely to be exacerbated by water repellency, as it decreases infiltration rates, enhances overland flow and increases the risk of soil erosion (Cerdà *et al.*, 1998; Doerr *et al.*, 2000). Water repellency is a transient soil property, which tends to be both spatially and temporally highly variable. It often disappears after periods of prolonged soil wetting, but will usually re-emerge during drier periods when soil moisture falls below a critical threshold (Dekker *et al.*, 2001). Water flow paths, once created, persist over time during summer, but over annual cycles their spatial arrangements can change completely (Wessolek *et al.*, 2009). Slight reductions in soil water content are known to cause substantial reductions in soil wettability (Czachor *et al.*, 2010). Soil water repellency is caused mainly by long-chained amphiphilic molecules, which have both hydrophilic (with polar functional group) and hydrophobic (with non-polar hydrocarbon chain) ends. Amphiphilic molecules may be released from a wide range of plants, organisms, and decaying organic matter. On drying, the hydrophilic ends bond more strongly with each other and soil particles, leaving an exposed hydrophobic surface (Hallett, 2007), leading to the fluctuations described previously. Both the persistence and severity of water repellency are influenced by land use and plant cover, as well as soil temperature, texture, pH, water content, and by soil organic carbon (SOC) and clay (mainly kaolinite) content (Doerr *et al.*, 2000; Dekker *et al.*, 2001; Lichner *et al.*, 2002; Arcenegui *et al.*, 2008; Lachacz *et al.*, 2009; Novák *et al.*, 2009; Diehl *et al.*, 2010). Wang *et al.* (2010) revealed that the wettability in water repellent soils was affected more by SOC than by soil texture and pH, whereas in wettable soils, soil texture and pH had a greater impact.

In grassland soils, wettability and infiltration can be affected considerably by vegetation cover (Alaoui *et al.*, 2011; Kodešovà *et al.*, 2011). Infiltration is a critical process in grasslands where resources such as water, litter, nutrients and biological activity are typically scaled at the level of individual plants (Schlesinger *et al.*, 1996). In general, the enhancement of infiltration due to plants and soil animal activity can be expected in fine-textured soils, whereas plants and biological crusts are known to decrease infiltration in coarse-textured soils (Cerdà, 1999; Ravi *et al.*, 2007; Caldwell *et al.*, 2008; Capuliak *et al.*, 2010; Cerdà and Doerr, 2010; Eldridge *et al.*, 2010). Grass cover can induce water repellency in all soil types ranging from sands (Dekker *et al.*, 2001) to clays (Dekker and Ritsema, 1996) by both root exudates and thatch (the layer of organic matter between the mineral soil and the green grass). In well-structured soils, roots are often found in the inter-aggregate pore network, and therefore, water repellent substances are found upon the faces of aggregates and/or larger structural elements (Gerke and Köhne, 2002). Repellency is generally absent within aggregates and larger structural elements where roots are absent (Dekker and Ritsema, 1996). Aamlid *et al.* (2009) found sand layers to be more strongly water repellent than the overlying organic thatch layer. This could be caused by leaching of amphiphilic compounds from litter and the organic layer, by grass root exudates, and/or by the hyphae and exudates of soil fungi (Bond, 1964).

The objective of the research was to quantify the influence of grass cover on hydrophysical parameters and heterogeneity of water flow in a sandy soil emerging during a heavy rain following a long hot, dry period. We hypothesised that soil water repellency, induced by the thatch and mucilages of grasses, as well as infilling of voids by organic matter, would reduce substantially sorptivity, and unsaturated and saturated hydraulic conductivity. Soil water repellency should also result in an increase in the heterogeneity of water flow (fingered flow). The practical relevance of our research is in quantifying the influence of grass cover on both the soil properties and the heterogeneity of water flow in a sandy soil.

MATERIALS AND METHODS

Study area

The field sites were located in the Borská nížina Lowland of southwest Slovakia. This area covers about

410 km^2 and consists of aeolian sand dunes. The region is in transition zone between temperate oceanic and continental climates. Precipitation is seasonal, averages 550 mm per year and is mainly summer-dominant. The climate in summer tends to consist of long hot and dry spells interspersed with intense rainfall. Air temperature averages about 9 °C. Temperatures of 50 °C on the surface of bare soil at a glade lasted about 5 hours a day during a hot summer, as measured on July 28, 2005. The daily precipitation amounts and temperature measured in the Meteorological Station of the Slovak Hydrometeorological Institute in Moravsky Svaty Jan, at a distance of about 5 km from the study sites, in July 2008 and 2010 are shown in Fig. 1.

The study area was located at Mlaky II near Sekule (48° 37′ 10″ N, 16° 59′ 50″ E) which is about 150 m a.s.l. Two sites, separated by a distance of about 50 m, formed the basis of our study. A control soil (pure sand) with limited impact of vegetation or organic matter was obtained by sampling at 50 cm depth beneath a glade area. This was compared to a grassland soil that was covered by a 10 cm thick humic layer and colonised by grasses (*Calamagrostis epigejos*, and *Agrostis tenuis*). The sand soil at the glade site supported a sparse cover of mosses (mainly *Polytrichum piliferum*) and lichens (mainly *Cladonia* sp.), and occasionally, grasses (mainly *Corynephorus canescens*) (Šomšák *et al.*, 2004). Some areas in the glade had exposed bare soil. Both the macroscopic and microscopic soil fungi have been recorded at this site (Lichner *et al.*, 2007).

The soil was a Regosol formed from windblown sand (IUSS Working Group WRB, 2006) and had a sandy texture (Soil Survey Division Staff, 1993). Physical and chemical properties of soil samples are presented in Table I. With the exception of organic carbon content (responsible for the differences in soil wettability), soil properties were almost identical. The mineralogy of the aeolian sand was primarily siliceous sand (silica content up to 90%), with a low content of primary minerals (feldspars and micas) (Kalivodová *et al.*, 2002). Compared with the 10-cm thick humic layer at the grassland soil, a thin humic layer a few milimeters thick occurred below the moss cover in the glade soil. The soil beneath this thin humic layer is wettable all year round. Thin textural transitions as well as an accumulation of Fe-oxides and Fe-hydroxides were detected in a 1–2 cm thick layer in the soil profiles during excavation (Lichner *et al.*, 2010).

Field methods

Soil water content was estimated by the gravime-

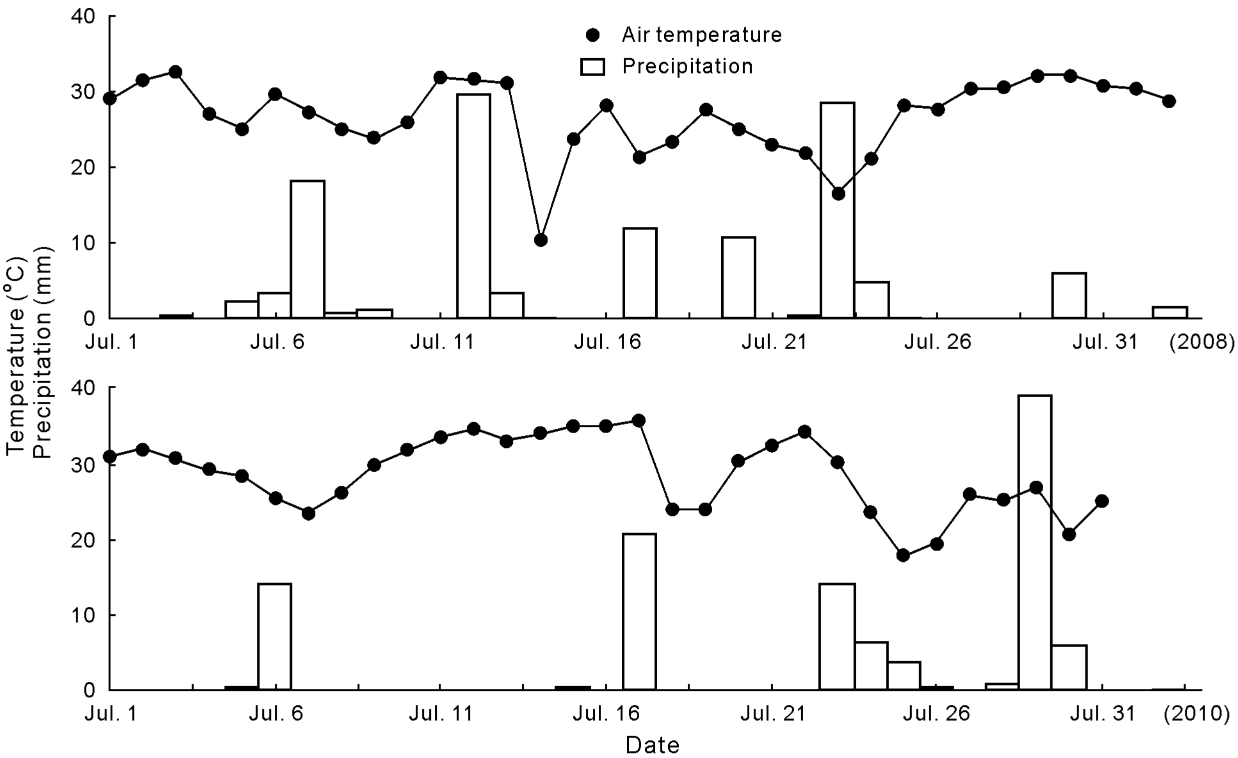

Fig. 1 Mean daily air temperatures and daily precipitations measured at the Meteorological Station of the Slovak Hydrometeorological Institute in Moravsky Svaty Jan (southwest Slovakia) in July–August 2008 and 2010.

TABLE I

Physical and chemical properties of the soil from the studied site

Site	Depth	Sand	Silt	Clay	$CaCO_3$	C	pH(H_2O)	pH(KCl)
	cm		%			g kg^{-1}		
Grassland	0–5	91.26	2.81	5.93	< 0.5	9.9	5.14	3.91
Pure sand	50–55	94.86	1.74	3.40	< 0.5	0.3	5.54	4.20

tric method after drying at 105 °C (Kutilek and Nielsen, 1994). The persistence of water repellency was measured using the water drop penetration time (WDPT) test (Doerr, 1998). In this study, 58 ± 5 μL drops of distilled water were placed onto the soil surface from a standard height of 10 mm above the surface, and the time required for infiltration was recorded.

Field measurements of infiltration were performed using a mini disk infiltrometer (Decagon Devices, USA) under a negative tension $h_0 = -196$ Pa. The mini disk infiltrometer had a diameter of 4.5 cm with liquid transport through sintered stainless steel disc at the base that was in contact with the soil. Measurements were made with water and ethanol, with the latter providing an infiltration measurement that was not influenced by water repellency.

The cumulative infiltration I was calculated based on the Philip infiltration equation (Philip, 1957):

$$I = C_1 t^{1/2} + C_2 t + C_3 t^{3/2} + C_4 t^2 + \ldots \tag{1}$$

where C_1, C_2, C_3, $C_4, \ldots$ are coefficients, and t is time.

Zhang (1997) proposed to estimate the sorptivity $S(h_0)$ and unsaturated hydraulic conductivity $k(h_0)$ at suction $h_0 \leq 0$ from:

$$I = C_1(h_0)t^{1/2} + C_2(h_0)t \tag{2}$$

where $C_1(h_0)$ and $C_2(h_0)$ are functions of suction h_0. The sorptivity $S(h_0)$ and unsaturated hydraulic conductivity $k(h_0)$ at suction $h_0 \leq 0$ can be calculated from:

$$S(h_0) = C_1(h_0)/A_1 \tag{3}$$

and

$$k(h_0) = C_2(h_0)/A_2 \tag{4}$$

where A_1 and A_2 are dimensionless coefficients. Eq. 3 was used to calculate the sorptivities of both water, $S_w(-196$ Pa), and ethanol, $S_e(-196$ Pa), from the cumulative infiltration *vs.* time relationships taken with the mini disk infiltrometer during early-time (< 180 s) infiltration of water and ethanol, respectively. The index of water repellency R was calculated from (Hallett *et al.*, 2001):

$$R = 1.95 S_e(-196\ \mathrm{Pa})/S_w(-196\ \mathrm{Pa}) \tag{5}$$

Eq. 4 was used to estimate the hydraulic conductivity $k(-196$ Pa) in this study, using $A_2 = 1.8$ for sandy soil and suction $h_0 = -196$ Pa from Table II in the Mini Disk Infiltrometer User's Manual, Version 6 (Decagon Devices, 2007). In our former calculations we used $A_2 = 2.4$ for sandy soil and suction $h_0 = -196$ Pa from the Mini Disk Infiltrometer User's Manual, Version 2, published in 2005, and this coefficient was changed to $A_2 = 1.73$ in Version 8, published in 2010. Dohnal *et al.* (2010) modified the original Zhang (1997) formula to lower the relative error of the hydraulic conductivity estimates. Grass and crust cover was removed (scalped) before the measurements of WDPT, $k(-196$ Pa), $S_w(-196$ Pa), and $S_e(-196$ Pa). Scalping could result in an increase in some of these properties, as observed by Eldridge *et al.* (2000) for sorptivity and steady-state infiltration rate under both ponding and tension.

Field measurements of infiltration under a small positive pressure head $h_0 = 196$ Pa were also performed repeatedly at all sites using a double-ring infiltrometer with an inner-ring diameter of 24.5 cm, buffer ring diameter of 34.5 cm, and length of 23.5 cm. The first two and three terms of the Philip infiltration equation (Eq. 1) can be used to estimate the saturated hydraulic conductivity K_s. The first two terms are applicable to relatively short times as follows:

$$I \approx S_w t^{1/2} + m K_s t \tag{6}$$

where S_w is the sorptivity of water, with coefficient $m = 0.667$ being the most frequently used value (Kutilek and Nielsen, 1994).

Kutílek and Krejča (1987) proposed to use three terms of the Philip infiltration equation to estimate the saturated hydraulic conductivity K_s:

$$K_\mathrm{s} \approx (3C_1C_3)^{1/2} + C_2 \tag{7}$$

Eqs. 6 and 7 were used to estimate the saturated hydraulic conductivity K_s in this study.

The tracer experiment at the grassland site was carried out at the 100 cm × 100 cm plot using the method similar to Bachmair *et al.* (2009) and Homolák *et al.* (2009). First, the grass was mowed, and the plot was partitioned into two smaller subplots (50 cm × 100 cm each) to apply different rainfall amounts (20 and 70 mm). Rainfall of 70 mm was chosen to represent increased rainfalls expected as a consequence of the climate change. Brilliant blue dye was added at a concentration of 10 g L^{-1} to the water used to simulate rainfall and the dyed water was applied at a rate of about 1 mm min^{-1}. The tracer application was conducted manually with a watering can, and it took 20 and 60 minutes for application amounts 20 mm (on the 100 cm × 100 cm plot) and next 50 mm (on the 50 cm × 100 cm subplot), respectively. Thirty minutes after the first sprinkling, vertical sections were excavated at distances of 15, 20, 30, and 40 cm from the edge of the plot, and clean soil profiles were photographed with a digital camera. Similarly, 30 minutes after the second sprinkling, vertical sections were excavated at distances of 60, 70, 80, 90, and 100 cm from the edge of the plot, and clean soil profiles were photographed.

The tracer experiment in the pure sand was carried out at the 50 cm × 100 cm plot, where 50 mm of dyed water was applied. The soil surface on this plot was flattened to prevent uneven infiltration of water due to ponding. The water dyed with brilliant blue was applied manually with a watering can at a rate of about 1 mm min^{-1}. Seventy minutes after sprinkling, vertical sections were excavated at distances of 10, 20, 30, 40, and 50 cm from the edge of the plot, and clean soil profiles were photographed with a digital camera. All the two-dimensional pictures were then digitally corrected and georeferenced using standard GIS software according to the scales provided.

To make dye patterns comparable among sites and rainfall amounts, two parameters were chosen for a characterization of vertical flow patterns: the effective cross section for water flow, ECS, and the degree of preferential flow, DPF. ECS was used to quantify the heterogeneity of water flow in soil. The approach presented in Täumer *et al.* (2006) was modified so that the fraction of total water content change was determined from the stained area. The picture of each vertical section was divided into $i = 10$ vertical bands with the width of 10 cm, and the numbers n_i of stained 5 cm × 5 cm pixels were calculated in each band. The number of stained pixels is not an integer if all the area of pixels was not stained. The fraction of total water content change f_i, which is the ratio between the water content change in band i and the total water content change in vertical profile, was calculated for each band using

$$f_i = n_i \Big/ \sum_{i=1}^{i=10} n_i \quad \text{with} \quad \sum_{i=1}^{i=10} f_i = 1 \tag{8}$$

The fractions f_i were ranked in descending order and presented against the fraction of cross-sectional area, FCA (black dots in Figs. 2b and 3b). A beta distribution

$$p(x,\alpha,\beta) = \frac{\Gamma(\alpha+\beta)}{\Gamma(\alpha)\Gamma(\beta)} x^{(\alpha-1)}(1-x)^{\beta-1} \qquad (\alpha>0,\ \beta>0,\ 0 \le x \le 1) \tag{9}$$

was fitted to the data and the Levenberg-Marquardt algorithm (the non-linear least-square fitting) was used to optimize the parameters α and β. The Levenberg-Marquardt method is a popular alternative to the Gauss-Newton method of finding the minimum of a function that is a sum of squares of nonlinear functions. The fitted curve expresses the share of the water content changes as a function of the area share. According to the definition in Täumer *et al.* (2006), ECS was then estimated as the fraction of the total area that corresponds to the 90% of water content change in vertical section (Figs. 2 and 3). ECS equals to 0.9 for piston flow, and it decreases with an increase in the impact of preferential flow on solute/dye transport in soils.

The degree of preferential flow, equal to the area between the beta distribution curve and the 1:1 line (the line represents the distribution of fraction of total water content change *vs.* fraction of cross-sectional area for a piston flow), was also used to quantify the heterogeneity of water flow in soil (Figs. 2 and 3). The DPF was calculated from

$$\mathrm{DPF} = \int_{x=0}^{1} p(x,\alpha,\beta) - 0.5 \tag{10}$$

DPF can change from 0 for piston flow to almost 0.5 for the case when all the flow in soil is realized through a narrow preferential path (*e.g.*, a crack in heavy clay soil).

A Student t-test (Matlab) was used to determine whether the data (WDPT, $S_\mathrm{w}(-196\ \mathrm{Pa})$, $S_\mathrm{e}(-196\ \mathrm{Pa})$, R, $k(-196\ \mathrm{Pa})$, K_s Eq. 6, K_s Eq. 7, ECS and DPF) dif-

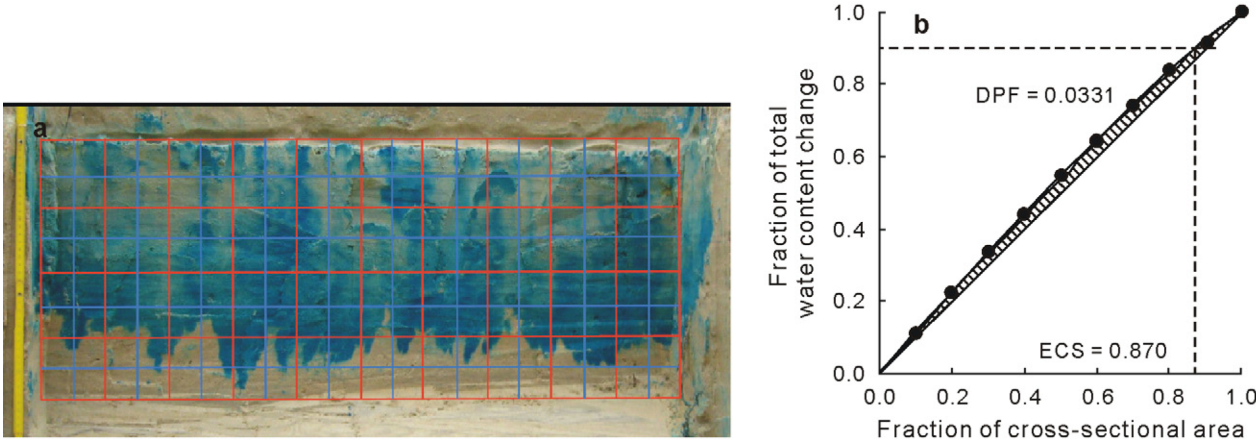

Fig. 2 Estimation of effective cross section (ECS) and degree of preferential flow (DPF) from the image of vertical section of dyed soil, taken in pure sand at the distance of 30 cm from the front edge during the 2008 tracer experiment. (a) The image of vertical section with 10 cm (red lines) and 5 cm (blue lines) grids used for an estimation of the fractions of total water content change; and (b) the plot of the cumulative water content changes against the cumulative cross-sectional area (black dots), with ECS estimated as the fraction of the total cross-sectional area that corresponds to the 90% of total water content change, and DPF presented as the shaded area between beta-function fitted to the data and straight line representing the piston flow.

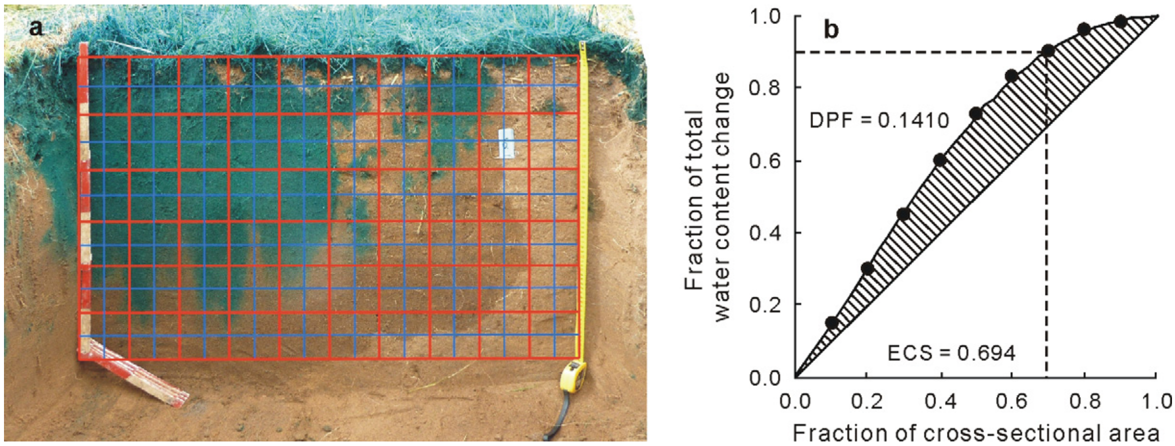

Fig. 3 Estimation of effective cross section (ECS) and degree of preferential flow (DPF) from the image of vertical section of dyed soil, taken in grassland soil at the distance of 60 cm from the front edge during the 2010 tracer experiment. (a) The image of vertical section with 10 cm (red lines) and 5 cm (blue lines) grids used for an estimation of the fractions of total water content change; and (b) the plot of the cumulative water content changes against the cumulative cross-sectional area (black dots), with ECS estimated as the fraction of the total cross-sectional area that corresponds to the 90% of total water content change, and DPF presented as the shaded area between beta-function fitted to the data and straight line representing the piston flow.

fered significantly between the two sites. Levene's test (Levene, 1960) was used to test whether the data were normally distributed with homogenous variances. The data that did not pass the test were transformed using the Box-Cox method based on estimation and minimization of standard deviation of the function under underlying transformation. Then, the t-test was used to compare the means and variances of the above data from the two sites to find out whether they were statistically significantly different.

RESULTS AND DISCUSSION

Impact of grass on hydrological properties of sandy soil

The hydrological properties of the soil at both sites are presented in Table II. It should be noted that one of eight estimates of K_s from Eq. 7 in pure sand and two of 10 estimates of K_s from Eq. 7 in grassland soil were rejected because the C_1C_3 product in Eq. 7 was negative.

TABLE II

Statistical parameters of hydrophysical properties for the two studied sites

Site	Attribute[a)]	Minimum	Maximum	Median	Arithmetic mean	Standard deviation	n[b)]
Grassland soil	WDPT (s)	1	2 640	75	347**	645	39
	$k(-196$ Pa) (m s^{-1})	1.67×10^{-6}	1.08×10^{-4}	3.73×10^{-5}	2.58×10^{-5}**	3.18×10^{-5}	10
	$S_w(-196$ Pa) (m s$^{-1/2}$)	7.40×10^{-5}	1.44×10^{-3}	5.56×10^{-4}	5.30×10^{-4}**	4.11×10^{-4}	10
	$S_e(-196$ Pa) (m s$^{-1/2}$)	9.97×10^{-4}	1.86×10^{-3}	1.08×10^{-3}	1.15×10^{-3}**	2.61×10^{-4}	10
	R	1.60	26.6	4.94	8.42*	8.67	10
	K_s Eq. 6 (m s^{-1})	6.40×10^{-5}	1.24×10^{-4}	7.44×10^{-5}	8.56×10^{-5}**	2.23×10^{-5}	10
	K_s Eq. 7 (m s^{-1})	1.68×10^{-5}	1.13×10^{-4}	2.96×10^{-5}	4.42×10^{-5}*	3.04×10^{-5}	8
	ECS (m^2 m^{-2})	0.694	0.858	0.800	0.795*	0.0583	8
	DPF	0.0464	0.1520	0.1280	0.0996*	0.0428	8
Pure sand	WDPT (s)	1	1		1**	0	39
	$k(-196$ Pa) (m s^{-1})	1.45×10^{-4}	7.80×10^{-4}	4.61×10^{-4}	4.78×10^{-4}**	2.17×10^{-4}	9
	$S_w(-196$ Pa) (m s$^{-1/2}$)	2.93×10^{-3}	1.17×10^{-2}	7.13×10^{-3}	7.60×10^{-3}**	2.95×10^{-3}	9
	$S_e(-196$ Pa) (m s$^{-1/2}$)	9.97×10^{-4}	3.98×10^{-3}	2.78×10^{-3}	2.68×10^{-3}**	8.76×10^{-4}	9
	R	0.28	1.85	0.644	0.816*	0.498	9
	K_s Eq. 6 (m s^{-1})	3.32×10^{-4}	7.04×10^{-4}	5.31×10^{-4}	5.23×10^{-4}**	1.37×10^{-4}	8
	K_s Eq. 7 (m s^{-1})	2.50×10^{-4}	1.51×10^{-3}	2.93×10^{-4}	5.14×10^{-4}*	4.46×10^{-4}	7
	ECS (m^2 m^{-2})	0.839	0.882	0.874	0.868*	0.0164	5
	DPF	0.0249	0.0574	0.0331	0.0364*	0.0132	5

*, ** denote significant differences between the soils at $P < 0.05$, and $P < 0.01$, respectively.
[a)] WDPT = water drop penetration time; k = hydraulic conductivity; S_w = sorptivity of water; S_e = sorptivity of ethanol; R = index of water repellency; K_s = saturated hydraulic conductivity; ECS = effective cross section for water flow; DPF = degree of preferential flow; (-196 Pa) = under a negative tension $h_0 = -196$ Pa.
[b)] n is the number of replicates.

Overall, our study demonstrated significant differences in hydrological properties between a sandy soil dominated by grasses and pure sand with negligible impact of biological factors. In general, the grassland soil was substantially more water repellent and exhibited lower values of sorptivity (under both water and ethanol), hydraulic conductivity and saturated hydraulic conductivity (Table II). In addition it had 3 times the degree of preferential flow than pure sand. The results of this study reinforced our view that the consequences of any change in climate, which will ultimately influence hydrology, will be markedly different between grasslands and bare soils.

In the grassland site, relatively low rates of sorptivity (the initial wetting up phase), even under the ethanol treatment, could have been due to a number of factors, but was most likely a result of the hydrophobic surface. The grassland soil had an index of water repellency 10 times that of pure sand (Table II). Even after the soil wetted up after the sorptivity phase, both hydraulic conductivity and saturated hydraulic conductivity were quite low for functional grasslands. The sandy soil in our study site had a very low percentage of fine material (3%–6% clay; Table I), making it structurally poor in the surface horizon where the macroporosity status is also likely low. Physical crusting is therefore likely to be common on these coarse-textured soils. Low levels of poorly aggregated silts and clays could also block the matrix pores, restricting water flow (Eldridge *et al.*, 2002).

Lower levels of saturated hydraulic conductivity in the grassland soil compared with pure sand could result from both almost 2 times higher silt and clay contents and more than 30 times higher content of organic carbon. This is consistent with findings of Blackburn (1975), Ravi *et al.* (2007) and Yan *et al.* (2010) that silt and clay content is negatively correlated with infiltration rates, as well as with findings of Wang *et al.* (2009) that soil carbon is negatively correlated with saturated hydraulic conductivity in a sandy soil.

Although we compared different variables estimated from the infiltration rate measured under different tensions, the coefficient of variation was inversely proportional to the volume of grassland soil, V. It was smallest for the measurements with the double-ring infiltrometer ($V \approx 35\,000$ cm^3), larger for the mini disk infiltrometer ($V \approx 80$ cm^3), and largest for the WDPT test ($V \approx 0.01$ cm^3). This is consistent with findings of Mallants *et al.* (1997) for spatial variability of saturated hydraulic conductivity in soil with extensive macropores.

Overall, the DPF was negatively related to ECS (DPF = −0.551 ECS + 0.5060, $R^2 = 0.993$).

Infiltration into pure sand

The tracer experiment was carried out on August 2, 2008. Gravimetric soil water content of pure sand in the depth of 50–55 cm was 72 g kg^{-1}. The wetting front (Fig. 2a) exhibited a form typical of that for stable flow with "air-draining" condition, when the soil air is allowed free to drain from ahead of the wetting front through an air exit at the bottom (Wang *et al.*, 2000). A lack of preferential flow is confirmed by the magnitude of the effective cross section which ranged from 0.839 to 0.882, and the degree of preferential flow which ranged from 0.0249 to 0.0574. The fraction of total water content change presented against the fraction of cross-sectional area at the distance of 30 cm from the front edge is shown in Fig. 2b, together with the values of ECS = 0.870 and DPF = 0.0331.

Infiltration into grassland soil

The tracer experiment was carried out on July 26, 2010. Total precipitation during 3 days preceding the experiment was 24.1 mm (Fig. 1). This represents relatively wet conditions for the study site. Gravimetric soil water contents were 98 and 121 g kg^{-1} for samples taken from the stained area, 76 and 119 g kg^{-1} for the soils wetted by previous rainfall, and 13 and 18 g kg^{-1} for the soils in the dry area, for the subplots irrigated by 20 and 70 mm of water, respectively. During the tracer experiments, we observed that surface water pooled into small micro-depressions. The shape of the wetting front taken at a distance of 60 cm from the leading edge and after 70 mm of infiltration (Fig. 3a) was similar to that of the unstable fingered flow with air-confined condition (Wang *et al.*, 2000). Based on the ponded area observed during water application, we attribute the columnar shape (Morales *et al.*, 2010) of the wetting front in the grassland to redistribution of applied water on the surface to the series of micro-catchments, which acted as runon and runoff zones. Our previous laboratory research on the grassland soils demonstrated a strong negative relationship between ponding depth/tension, h (49 to 294 Pa) and the time to commencement of infiltration, t_c (min) ($t_c = 52.6 - 16.6\ h$, $P = 0.006$, $R^2 = 0.878$) (Lichner *et al.*, 2010). In the field, however, perennial grass butts can reduce this time as they are capable of soaking up substantial quantities of ponded water (Bochet *et al.*, 2000). Cryptogamic crusts on grassy slopes can also contribute to this patchwork of small runoff zones (Eldridge, 1993).

The well-developed preferential flow at this site was evident from the values of effective cross-section, which ranged from 0.694 to 0.858, and the values of the degree of preferential flow, which ranged from 0.0464 to 0.152. The fraction of total water content change presented against the fraction of cross-sectional area at the distance of 60 cm from the front edge is shown in Fig. 3b, together with the values of ECS = 0.694 and DPF = 0.1410.

Our data showed, however, the overriding effect of water repellency on these grassland soils, which had a variable cover of biological crusts. Research worldwide has shown that infiltration is substantially greater under grasses than in the interspaces (*e.g.*, Eldridge *et al.*, 2010). Our study, however, did not separate hydrological processes over the grass butts themselves and in the interspaces. Similarly we did not expect high levels of infiltration on the moss and lichen covered surface given the general observation that crusts enhance runoff (*e.g.* Eldridge *et al.*, 2002). However, the effects of biological crusts on infiltration processes vary between studies, with reports of enhanced (Gifford, 1972; Blackburn, 1975) and reduced infiltration depending on the situation. One potential mechanism is that crusts could maintain the structural integrity of the soil surface by preventing the formation of physical raindrop-impact crusts, which are known to reduce infiltration (Valentin, 1991). Similar mechanisms have been observed in arid *Stipa*-dominant grasslands in Spain (Eldridge *et al.*, 2010). Crusts would be expected to retain small amounts of water within microcracks and depressions would pond water and increase infiltration. This could explain some of the difference in infiltration capacity between the two sites.

Small amounts of litter and plant cover on the coarse-textured soils may not have been sufficient to protect the soil against raindrop action and prevent surface crusting. The situation on the sandy moss covered soils, however, may have been quite different, with even sparse mosses and lichens maintaining the structural stability and providing entry points for infiltration. More likely, however, is that the general absence of a thatch layer on the non-grassy sites was insufficient to induce water repellency.

CONCLUSIONS

Our results support the notion that biotic processes have substantial effects on soil hydrology. The marked difference in infiltration capacity between grassy and sparsely covered moss-dominant sites reinforces our view that we must consider the relative proportion of water-repellent grassland sites and adjacent moss-dominant sites to fully appreciate the nature of the hydrological response in this environment. Saturated hydraulic conductivity values in the grasslands and sandy areas ranged from 230–2 500 mm h^{-1}, far in excess of the maximum rainfall intensity likely in the study area. More detailed studies are required, however, to examine larger (and smaller) scale processes of runoff and infiltration in these grasslands.

REFERENCES

Aamlid, T. S., Espevig, T. and Kvalbein, A. 2009. The potential of a surfactant to restore turfgrass quality on a severely water-repellent golf green. *Biologia.* **64**: 620–623.

Alaoui, A., Caduff, U., Gerke, H. H. and Weingartner, R. 2011. Preferential flow effects on infiltration and runoff in grassland and forest soils. *Vadose Zone J.* **10**: 367–377.

Arcenegui, V., Mataix-Solera, J., Guerrero, C., Zornoza, R., Mataix-Beneyto, J. and García-Orenes, F. 2008. Immediate effects of wildfires on water repellency and aggregate stability in Mediterranean calcareous soils. *Catena.* **74**: 219–226.

Bachmair, S., Weiler, M. and Nützmann, G. 2009. Controls of land use and soil structure on water movement: Lessons for pollutant transfer through the unsaturated zone. *J. Hydrol.* **369**: 241–252.

Blackburn, W. H. 1975. Factors influencing infiltration and sediment production of semi-arid rangelands in Nevada. *Water Resour. Res.* **11**: 929–937.

Bochet, E., Poesen, J. and Rubio, J. L. 2000. Mound development as an interaction of individual plants with soil, water erosion and sedimentation processes on slopes. *Earth Surf. Proc. Land.* **25**: 847–867.

Bond, R. D. 1964. The influence of the microflora on the physical properties of soils. II. Field studies on water repellent sands. *Aust. J. Soil Res.* **2**: 123–131.

Caldwell, T. G., Young, M. H., Zhu, J. T. and McDonald, E. V. 2008. Spatial structure of hydraulic properties from canopy to interspace in the Mojave Desert. *Geophys. Res. Lett.* **35**: L19406.

Capuliak, J., Pichler, V., Flühler, H., Pichlerová, M. and Homolák, M. 2010. Beech forest density control on the dominant water flow types in Andic soils. *Vadose Zone J.* **9**: 747–756.

Cerdà, A. 1999. Parent material and vegetation affect soil erosion in eastern Spain. *Soil Sci. Soc. Am. J.* **63**: 362–368.

Cerdà, A. and Doerr, S. H. 2010. The effect of ant mounds on overland flow and soil erodibility following a wildfire in eastern Spain. *Ecohydrology.* **3**: 392–401.

Cerdà, A., Schnabel, S., Gomez-Amelia, D. and Ceballos, A. 1998. Soil hydrological response under simulated rainfall in the Dehesa ecosystem, Extremadura, SW, Spain. *Earth Surf. Proc. Land.* **23**: 195–209.

Czachor, H., Doerr, S. H. and Lichner, L. 2010. Water retention of repellent and subcritical repellent soils: new insights from model and experimental investigations. *J. Hydrol.* **380**: 104–111.

Decagon Devices. 2007. Mini Disk Infiltrometer—User's Manual. Version 6. Decagon Devices, Inc., Pullman.

Dekker, L. W. and Ritsema, C. J. 1996. Preferential flow paths in a water repellent clay soil with grass cover. *Water Resour. Res.* **32**: 1239–1249.

Dekker, L. W., Doerr, S. H., Oostindie, K., Ziogas, A. K. and Ritsema, C. J. 2001. Water repellency and critical soil water content in a dune sand. *Soil Sci. Soc. Am. J.* **65**: 1667–1674.

Diehl, D., Bayer, J. V., Woche, S. K., Bryant, R., Doerr, S. H. and Schaumann, G. E. 2010. Reaction of soil water repellency to artificially induced changes in soil pH. *Geoderma.* **158**: 375–384.

Doerr, S. H. 1998. On standardizing the 'Water Drop Penetration Time' and the 'Molarity of an Ethanol Droplet' techniques to classify soil hydrophobicity: a case study using medium textured soils. *Earth Surf. Proc. Land.* **23**: 663–668.

Doerr, S. H., Shakesby, R. A. and Walsh, R. P. D. 2000. Soil water repellency: its causes, characteristics and hydro-geomorphological significance. *Earth-Sci. Rev.* **51**: 33–65.

Dohnal, M., Dusek, J. and Vogel, T. 2010. Improving hydraulic conductivity estimates from minidisk infiltrometer measurements for soils with wide pore-size distributions. *Soil Sci. Soc. Am. J.* **74**: 804–811.

Eldridge, D. J. 1993. Cryptogam cover and soil surface condition: effects on hydrology on a semiarid woodland soil. *Arid Soil Res. Rehab.* **7**: 203–217.

Eldridge, D. J., Zaady, E. and Shachak, M. 2000. Infiltration through three contrasting biological soil crusts in patterned landscapes in the Negev, Israel. *Catena.* **40**: 323–336.

Eldridge, D. J., Zaady, E. and Shachak, M. 2002. Microphytic crusts, shrub patches and water harvesting in the Negev Desert: the *Shikim* system. *Landscape Ecol.* **17**: 587–597.

Eldridge, D. J., Bowker, M. A., Maestre, F. T., Alonso, P., Mau, R. L., Papadopoulos, J. and Escudero, A. 2010. Interactive effects of three ecosystem engineers on infiltration in a semi-arid Mediterranean grassland. *Ecosystems.* **13**: 499–510.

Faško, P., Lapin, M. and Pecho, J. 2008. 20-year extraordinary climatic period in Slovakia. *Meteorol. Časopis.* **11**: 99–105.

Gerke, H. H. and Köhne, J. M. 2002. Estimating hydraulic properties of soil aggregate skins from sorptivity and water retention. *Soil Sci. Soc. Am. J.* **66**: 26–36.

Gifford, G. F. 1972. Infiltration rate and sediment production on a ploughed big sagebrush site. *J. Range. Manage.* **25**: 53–55.

Hallett, P. D. 2007. An introduction to soil water repellency. *In* Gaskin, R. E. (ed.) Adjuvants for Agrochemicals. Hand Multimedia, Christchurch, New Zealand.

Hallett, P. D., Baumgartl, T. and Young, I. M. 2001. Subcritical water repellency of aggregates from a range of soil management practices. *Soil Sci. Soc. Am J.* **65**: 184–190.

Hardy, J. T. 2003. Climate Change. Causes, Effects, and Solutions. Wiley, Chichester.

Holko, L., Kostka, Z. and Šanda, M. 2011. Assessment of frequency and areal extent of overland flow generation in a forested mountain catchment. *Soil Water Res.* **6**: 43–53.

Homolák, M., Capuliak, J., Pichler, V. and Lichner, L. 2009. Estimating hydraulic conductivity of a sandy soil under different plant covers using minidisk infiltrometer and a dye tracer experiment. *Biologia.* **64**: 600–604.

IUSS Working Group WRB. 2006. World Reference Base for Soil Resources 2006. 2nd Edition. World Soil Resources Reports No. 103. FAO, Rome.

Kalivodová, E., Kubíček, F., Bedrna, Z., Kalivoda, H., Gavlas, V., Kollár, J., Gajdoš, P. and Štepanovičová, O. 2002. Sand Dunes of Slovakia (in Slovak). Luka Press, Bratislava.

Kodešová, R., Jirků, V., Kodeš, V., Mühlhanselová, M., Nikodem, A. and Žigová, A. 2011. Soil structure and soil hydraulic properties of Haplic Luvisol used as arable land and grassland. *Soil Till. Res.* **111**: 154–161.

Kutílek, M. and Krejča, M. 1987. Three-parameter infiltration equation of Philip type. *Vodohosp. Časopis* (in Czech). **35**: 52–61.

Kutilek, M. and Nielsen, D. R. 1994. Soil Hydrology: Texbook for Students of Soil Science, Agriculture, Forestry, Geoecology, Hydrology, Geomorphology and Other Related Disciplines. Catena Verlag, Cremlingen-Destedt.

Lachacz, A., Nitkiewicz, M. and Kalisz, B. 2009. Water repellency of post-boggy soils with a various content of organic matter. *Biologia.* **64**: 634–638.

Lenderink, G. and van Meijgaard, E. 2010. Linking increases in hourly precipitation extremes to atmospheric temperature and moisture changes. *Environ. Res. Lett.* **5**: 025208.

Levene, H. 1960. Robust tests for equality of variances. *In* Olkin, I. *et al.* (eds.) Contributions to Probability and Statistics. Stanford University Press, Palo Alto. pp. 278–292.

Lichner, L., Babejová, N. and Dekker, L. W. 2002. Effects of kaolinite and drying temperature on the persistence of soil water repellency induced by humic acids. *Rost. Výroba.* **48**: 203–207.

Lichner, L., Hallett, P. D., Feeney, D., Ďugová, O., Šír, M. and Tesař, M. 2007. Field measurement of the impact of hydrophobicity on soil water transport under different vegetation over time. *Biologia.* **62**: 537–541.

Lichner, L., Hallett, P. D., Orfánus, T., Czachor, H., Rajkai, K., Šír, M. and Tesař, M. 2010. Vegetation impact on the hydrology of an aeolian sandy soil in a continental climate. *Ecohydrology.* **3**: 413–420.

Mallants, D., Mohanty, B. P., Vervoort, A. and Feyen, J. 1997. Spatial analysis of saturated hydraulic conductivity in a soil with macropores. *Soil Technol.* **10**: 115–131.

Morales, V. L., Parlange, J.-Y. and Steenhuis, T. S. 2010. Are preferential flow paths perpetuated by microbial activity in the soil matrix? A review. *J. Hydrol.* **393**: 29–36.

Novák, V., Lichner, L., Zhang, B. and Kňava, K. 2009. The impact of heating on the hydraulic properties of soils sampled under different plant cover. *Biologia.* **64**: 483–486.

Pekarova, P., Konicek, A. and Miklanek, P. 1999. Testing of AGNPS model application in Slovak microbasins. *Phys. Chem. Earth Pt. B.* **24**: 303–305.

Philip, J. R. 1957. The theory of infiltration: 1. The infiltration equation and its solution. *Soil Sci.* **83**: 345–358.

Ravi, S., D'Odorico, P. and Okin, G. S. 2007. Hydrologic and aeolian controls on vegetation patterns in arid landscapes. *Geophys. Res. Lett.* **34**: L24S23.

Šanda, M. and Císlerová, M. 2009. Transforming hydrographs in the hillslope subsurface. *J. Hydrol. Hydromech.* **57**: 264–275.

Schlesinger, W. H., Raikes, J. A., Hartley, A. E. and Cross, A. F. 1996. On the spatial pattern of soil nutrients in desert ecosystem. *Ecology.* **77**: 364–374.

Soil Survey Division Staff. 1993. Soil Survey Manual. Soil Conservation Service. U.S. Department of Agriculture Handbook 18.

Solomon, S., Qin, D., Manning, M., Chen, Z., Marquis, M., Averyt, K. B., Tignor M. and Miller, H. L. (eds). 2007. Climate Change 2007: The Physical Science Basis: Contribution of Working Group I to the Fourth Assessment Report of the Intergovernmental Panel on Climate Change. Cambridge University Press, Cambridge.

Šomšák, L., Šimonovič, V. and Kollár, J. 2004. Phytocoenoses of pine forests in the central part of the Zahorska nizina Lowland. *Biologia.* **59**: 101–113.

Täumer, K., Stoffregen, H. and Wessolek, G. 2006. Seasonal dynamics of preferential flow in a water repellent soil. *Vadose Zone J.* **5**: 405–411.

Valentin, C. 1991. Surface crusting in two alluvial soils of northern Niger. *Geoderma.* **48**: 201–222.

Wang, T., Wedin, D. and Zlotnik, V. A. 2009. Field evidence of a negative correlation between saturated hydraulic conductivity and soil carbon in a sandy soil. *Water Resour. Res.* **45**: W07503.

Wang, X. Y., Zhao, Y. and Horn, R. 2010. Soil wettability as affected by soil characteristics and land use. *Pedosphere.* **20**: 43–54.

Wang, Z., Wu, Q. J., Wu, L., Ritsema, C. J., Dekker, L. W. and Feyen, J. 2000. Effects of soil water-repellency on infiltration rate and flow instability. *J. Hydrol.* **231–232**: 265–276.

Wessolek, G., Stoffregen, H. and Täumer, K. 2009. Persistency of flow patterns in a water repellent sandy soil Conclusions of TDR readings and a time-delayed double tracer experiment. *J. Hydrol.* **375**: 524–535.

Yan, F. L., Shi, Z. H., Cai, C. F. and Li, Z. X. 2010. Wetting rate and clay content effects on interrill erosion in Ultisols of southeastern China. *Pedosphere.* **20**: 129–136.

Zhang, R. 1997. Determination of soil sorptivity and hydraulic conductivity from the disk infiltrometer. *Soil Sci. Soc. Am. J.* **61**: 1024–1030.